Evidence of the Existence of Micelles in the Fibrillogenesis of β-Amyloid Peptide

Raimon Sabaté and Joan Estelrich*

Departament de Fisicoquímica, Facultat de Farmàcia, Universitat de Barcelona, Avda. Joan XXIII s/n, 08028 Barcelona, Catalonia, Spain

Received: February 9, 2005; In Final Form: April 8, 2005

Alzheimer's disease (AD) is characterized by the deposition of fibrillar deposits formed by the amyloid β (Aβ) peptide. The most widely accepted model of fibrillogenesis of Aβ affirms that fibrillogenesis occurs in two distinct stages, nucleation and elongation. A modification of the model includes the formation of micelles. We have demonstrated with accurate experimental determinations the existence of aggregates with micellar properties (namely, the critical micellar concentration, CMC, and aggregation number). Values of the CMC were obtained by analysis of surface tension (17.5 μM) and changes in the fluorescence of pyrene (17.6 μM), respectively. The average aggregation number determined by fluorescence quenching was 25, and it was independent of peptide concentration. The presence of micelles implies that above the CMC all excess peptide is incorporated into micelles, and consequently, the monomer concentration is kept almost constant. Thus, micelles act as a peptide reservoir. Micelles are located on-pathway, since they serves as nucleation centers. Experimental data support the model, since above 17.7 μM the time of half-aggregation is independent of peptide concentration, and the overall reaction of the conversion of monomer peptide into fibril can be treated as an apparent first-order reaction.

Introduction

Alzheimer's disease (AD) is a neurodegenerative disorder characterized by the progressive deposition of amyloid β (Aβ) peptide.[1] The Aβ is a 40−42 amino acids long polypeptide generated from a membrane protein called amyloid precursor protein. Aβ has an amphipathic sequence; the amino-terminal residues 1−28 are polar, and residues 29−40 (or 29−42) are hydrophobic. At physiological pH, Aβ bears six negative charges.

Although the causal relationship between AD and the development of Aβ deposits has yet to be proven, on the basis of two lines of circumstantial evidence, namely, the presence of Aβ fibrils in senile plaques and a correlation between the in vitro degenerative effects of Aβ and the age and fibrillar morphology of Aβ, the formation of Aβ fibrils is commonly believed to be causatively linked to AD.[2] This is the "amyloid hypothesis". Similar such conversions of soluble proteins or protein fragments into fibrillar polymers occur in diseases, the so-called conformational diseases, as diverse as Huntington's disease, senile systemic amyloidosis, transmissible spongiform encephalitis, and type II diabetes.[3] The pathogenesis of all conformational diseases involves conformational changes leading to aberrantly folded proteins, rich in β secondary structure, that have a high tendency to form aggregates.[4]

It is widely accepted that Aβ fibrillogenesis occurs in two distinct stages, nucleation and elongation of fibers, and that the kinetics of the process are controlled by two key parameters, nucleation (k_n) and elongation (k_e) rate constants.[5] This model is similar to a nucleation-dependent polymerization process, much like that which characterizes crystal growth. According to this model, unstructured monomers in solution cluster and form nuclei. Formation of a stable nucleus requires a series of association steps that are thermodynamically unfavorable, because the resultant intermolecular interactions do not outweigh the entropic cost of association. Thus, a monomer is very slowly converted to an *n*-mer nucleus, and a lag time (lag phase) is observed before aggregation occurs. According to this model, the length of the lag time should be very sensitive to protein concentration (the lag time must be proportional to $1/C_P^n$, where C_P is the peptide concentration and n is the number of molecules in the nucleus).[5] Once the nucleus has reached a critical size, it forms a fibril,[6,7] and the fibrils grow from nuclei through the addition of Aβ monomers to the ends. Fibrils can also nucleate on heterogeneous nuclei (seeds). The addition of monomers becomes thermodynamically favorable when monomers contact the growing polymer at multiple sites, resulting in rapid polymerization/growth (linear phase), until equilibrium is reached and fibril mass concentration no longer changes (plateau phase).[5,8] It has been suggested that this aggregated form may represent an absolute minimum of Gibbs free energy.[9] Although this model is based on the assumption that Aβ is monomeric in the reaction mixture, stable Aβ dimers, suggested by Soreghan et al.[10] and detected by Walsh et al.,[11] would also be consistent with this model. The lag phase can be eliminated by adding trace amounts of preformed aggregate as "seed" material, which induces aggregation immediately. Seeding apparently eliminates the need for de novo formation of aggregation nuclei. Analysis of the data in the context of a simple model of fibril nucleation and growth have suggested a first-order dependence of the elongation rate on Aβ concentration as well as a strong dependence of the elongation rate constant on temperature. [12] This view may be supplemented by the possibility that, above a certain critical concentration, Aβ monomers associate to form micelles and that those micelles may convert to fibril nuclei.[6,7] In this way, measurements carried out using small angle neutron scattering (SANS) have shown that, under acidic conditions, an aggregate exists, with an elongated geometry, which exhibits

* Author to whom correspondencs should be addressed. Phone: +34-93-4024559. Fax: +34-93-4035987. E-mail: joanestelrich@ub.edu.

10.1021/jp050716m CCC: $30.25
Published on Web 05/11/2005

SCHEME 1: Sequence of the Fragment (1−40) of the Peptide

$Asp^{1} - Ala^{2} - Glu^{3} - Phe^{4} - Arg^{5} - His^{6} - Asp^{7} - Ser^{8} - Gly^{9} - Tyr^{10} - Glu^{11} - Val^{12} - His^{13} - His^{14} - Gln^{15} - Lys^{16} - Leu^{17} - Val^{18} - Phe^{19} - Phe^{20} - Ala^{21} - Glu^{22} - Asp^{23} - Val^{24} - Gly^{25} - Ser^{26} - Asn^{27} - Lys^{28} - Gly^{29} - Ala^{30} - Ile^{31} - Ile^{32} - Gly^{33} - Leu^{34} - Met^{35} - Val^{36} - Gly^{37} - Gly^{38} - Val^{39} - Val^{40}$

an average hydrodynamic radius of 7 nm.[13] Kayed et al. have observed that soluble Aβ oligomers, which could be entities of micellar characteristics, are common to most amyloid and may represent the primary toxic species of amyloids.[14]

From the above considerations, it is evident that to gain a full understanding of the process of amyloid formation, it is crucial to establish whether micelles are present in the formation of fibrils of Aβ, since in the model including micelles the fibrillogenesis pathway differs depending upon whether the total protein concentration is above or below a certain critical concentration.[7] In consequence, the determination of the critical micellar concentration (CMC) as well as of the aggregation number will be of great importance to characterize the micelles. Furthermore, it is necessary to locate the position of the micelles in the fibrillogenesis process.

In this paper, we show that above a determined peptide concentration Aβ aggregates in a cluster with micellar properties. Moreover, in relation to the fibrillogenesis, micelles must be located on-pathway.

Experimental Section

Peptides. The fragment 1−40 of Aβ (Scheme 1) (trifluoroacetic acid salt) was obtained from Bachem (Bubendorf, Switzerland). A stock solution of peptide was prepared by dissolving 1 mg of Aβ in 500 μL of 1,1,1,3,3,3-hexafluoro-2-propanol (HFIP), which had been dried at 4 °C over Molecular Sieve Type 4A and then centrifuged (15 000*g* for 15 min) to remove molecular sieve dust. After the dissolution, the solution was incubated with stirring at room temperature for 1 h in sealed vials. Then, the solution was bath-sonicated for 30 min and stirred for 1 h at room temperature. After that, the solution was kept at 4 °C for 30 min to avoid solvent evaporation when aliquoting. Once the sample was aliquoted, the HFIP was removed by evaporation under a gentle stream of nitrogen, leaving a slightly yellow film that was resuspended in 50 μL of anhydrous dimethyl sulfoxide (DMSO) and bath-sonicated for 10 min. Sonication was crucial to remove any traces of undissolved seeds that may resist solubilization. Aliquots of Aβ were added to 850 μL of water and 100 μL of 100 mM Tris-HCl buffer, pH 7.4. The final buffer contained 10 mM Tris, pH 7.4 and 5% (v/v) DMSO.

Homogeneity of Aβ was confirmed by sodium dodecyl sulfate polyacrylamide gel elecrophoresis (SDS-PAGE). Aliquots of 0.5 or 1 μg dissolved in the buffer solution were heated to 95 °C for 6 min, subsequently electrophoresed on a 15% running gel and a 4% stacking gel, and stained with silver nitrate. For comparison, rainbow-colored protein markers (2350−46 000 kDa) (Amersham Biosciences, Sweden) were used.

Reagents. Molecular sieves (0.4 nm) and HFIP were from Sigma (St. Louis, MO). Pyrene was from Fluka (Buchs, Switzerland), and 1-dodecylpyridinium chloride hydrate (DCP) 98% was from Aldrich (Steinheim, Germany). Organic solvents, when possible of spectroscopic grade, were purchased from Merck (Darmstadt, Germany). Solutions were prepared in double-distilled water purified through a Milli-Q system (Millipore, USA).

Determination of CMC. We use the definition of CMC proposed by Phillips,[15] who defines CMC as the total concentration of surfactant (in our case of peptide, C_P) corresponding to the maximum change in the gradient of the physical property, ψ, versus the C_P function given in eq 1

$$\left(\frac{d^3\psi}{dC_P^{\,3}}\right)_{C_P=\mathrm{CMC}} = 0 \qquad (1)$$

According to this definition, CMC is commonly determined from the intercept of two straight lines fitting ψ versus the C_P function in the concentration ranges below and above the CMC.

The CMC of the Aβ was assessed by equilibrium surface pressure measurements as well as by changes in the intensity of the fluorescence of pyrene. In the first method,[16] the CMC was determined at room temperature (24 ± 1 °C) by the Wilhelmy plate method using a digital tensiometer (Nima Tensiometer, Coventry, U. K.). The atmosphere was nearly saturated with water by inserting beakers with water inside the measuring chamber. If there is adsorption of surface-active compounds at the interface, then the surface tension of the solution decreases. The difference,

$$\pi = \gamma_{\mathrm{solvent}} - \gamma_{\mathrm{solution}} \qquad (2)$$

is called the surface pressure of the film formed by the adsorbed molecules. Time precautions were taken to ensure that equilibrium was reached. The reproducibility of the surface tension was ±0.01 mN m^{-1}. In this assay, peptide solutions were prepared by diluting with the buffer (10 mM Tris-HCl, 5% DMSO, pH 7.4). In the second method,[17] the relative changes in the intensities of the vibronic bands (specifically the ratio of the fluorescence intensities of the first and the third bands) in the pyrene fluorescence spectrum as a function of Aβ concentration were used to calculate the CMC, since this ratio is very sensitive to the polarity of the environment. This assay was performed in an Aminco-Bowman luminiscence spectrometer (Urbana, IL).

Determination of the Aggregation Number. The aggregation number, *N*, was determined by fluorescence static quenching according to the Infelta−Tachiya formula.[18,19] The method involves labeling micelles with a fluorescent probe and measuring steady-state fluorescence before and after the addition of a second species, the quencher, which deactivates excited molecules of the probe species. The probe used was pyrene, and the quencher was the dodecylpyridinium ion; both are soluble in the micellar pseudo-phase. If the quenching is static, then fluorescence is observed only from micelles devoid of quenchers. Assuming a Poissonian distribution of the quencher molecules, the relationship between the fluorescence intensity and the average number of quenchers per micelle $\langle n \rangle$ is

$$\ln \frac{I_0}{I_Q} = \langle n \rangle \qquad (3)$$

where I_0 is the emission intensity at a certain wavelength in the absence of an added fluorescence quencher and I_Q is the intensity at the same wavelength in the presence of a quencher.

$\langle n \rangle$ is related to the micellar aggregation number, *N*, by the following relation[20]

$$\langle n \rangle = \frac{Q_m}{M} = \frac{Q_m N}{C_P - \mathrm{CMC}} \qquad (4)$$

where Q_m is the concentration of quencher in the micelles, M is the concentration of micelles, and C_P is the total concentration of peptide. We have previously confirmed that the quencher does not aggregate itself in micelles in the concentration range used, and therefore, the free concentration of quencher can be disregarded, then $Q_m \approx Q$, the total concentration of quencher. If the fluorescence intensities at various quencher concentrations with fixed peptide concentrations are measured and a logarithm of the intensity ratio (I_0/I_Q) at a specific wavelength within the spectral emission range is plotted against the quencher concentration Q, a straight line is obtained through the origin with a slope equal to $1/M$, according to eqs 3 and 4. Multiplying the slope by the concentration of peptide molecules participating in micelle formation (i.e., C_P − CMC) gives the aggregation number (eq 4). The intensity of band III in the pyrene emission spectrum was chosen ($\lambda \approx 338$ nm) to avoid scattering problems, which could occur if the intensity of band I (at 372 nm) was used.[21] We observed that the N values obtained from the above analysis depend on the quencher concentration. When any surface-active substance and quencher mix ideally in small micelles the "quencher average" aggregation number N is dependent upon the ratio Q_m/C_P according to Warren and Grieser.[22]

$$N = N_w - \frac{\sigma^2}{2}\frac{Q_m}{C_P} \tag{5}$$

where N_w is the weight average aggregation number and σ^2 is the variance of the weight distribution. N_w and the "polydispersity index" σ/N_w can be determined from a plot of N versus Q_m/C_P by fitting eq 5 to the data.

Spectrophotometry. For the aggregation assay, the absorbance at 275 (tyrosine peak plus scattering) or at 400 nm (scattering of the sample) was measured in a Shimadzu UV-2401 PC UV−vis spectrophotometer using a matched pair of quartz microcuvettes (1 cm optical length) placed in a temperature-controlled cell holder. Approximately 1 mL of the peptide solution was poured into a cuvette, which was then capped tightly and placed inside a temperature-controlled incubator containing a magnetic stirrer. The solutions were stirred continuously at 1500 rpm. The peptide solution was briefly mixed by vortexing before each absorbance measurement to suspend the fibrils formed. The temperature was maintained at 37 ± 0.1 °C. For any kinetic curve, the endpoint amplitude was measured, and the corresponding value of absorbance was assigned to correspond to a maximal amount of peptide in fibrillar form. Absorbance values obtained as a function of time were transformed into the fraction of fibrils formed in the system, f. According to Kamihira et al.,[23] a sigmoidal curve fits the following equation, used by us for the Aβ fibrillization[24]

$$f = \frac{\rho\{\exp[(1+\rho)kt] - 1\}}{\{1 + \rho\exp[(1+\rho)kt]\}} \tag{6}$$

under the boundary conditions of $t = 0$ and $f = 0$, where $k = k_e C_P$ and ρ represent the dimensionless values to describe the ratio of k_n to k. By nonlinear regression of f against t, values of ρ and k can easily be obtained and from them the rate constants, k_e and k_n. The units of the nucleation and elongation constants are s^{-1} and L mol^{-1} s^{-1}, respectively.

The extrapolation of the linear portion of the sigmoidal curve to the abscissa ($f = 0$) and to the highest ordinate value of the fitted plot afforded two values of time (t_0 and t_1), which correspond to the lag time and to the time at which the aggregation was almost complete (time of the endpoint amplitude). The time required to reach half-maximal amplitude (i.e., when $f = 0.5$) is the time of half-aggregation ($t_{1/2}$).

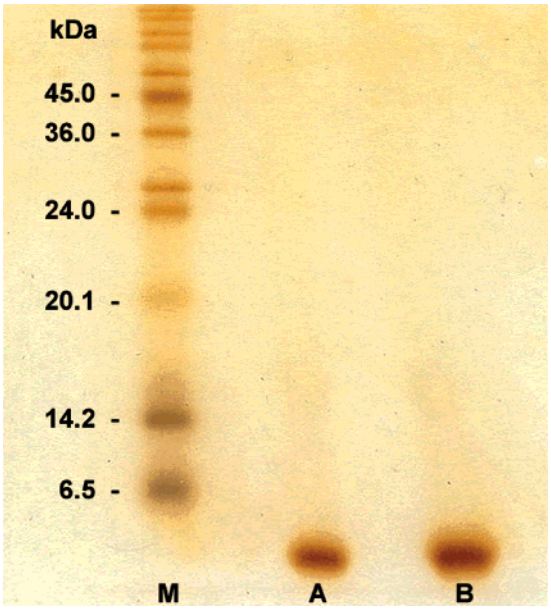

Figure 1. SDS-PAGE of Aβ. Sample: 0.5 μL (A) or 1.0 μL (B) of a 1 mg mL^{-1} solution. Protein markers (M): 5 μL (SigmaMarker Wide Range, M_r from 6500 to 205 000 kDa). The separation gel was 14% acrylamide/bisacrylamide. The bands were silver-stained.

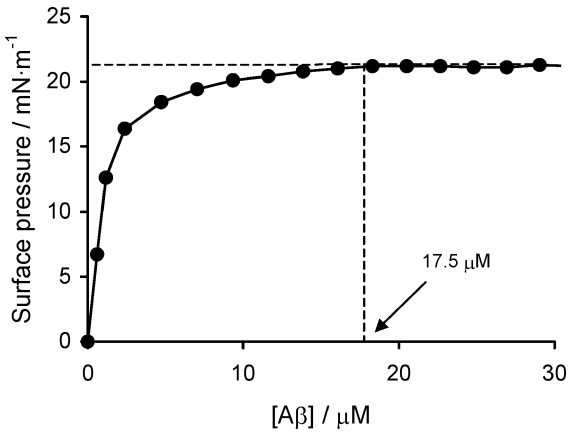

Figure 2. Surface pressure values as a function of peptide concentration. The surface pressure, π, measures the adsorption of peptides at the air/water interface. Each point is the mean value of five measurements. The standard deviations for the series of values are smaller than the sizes of the symbols.

Results

The physicochemical properties of Aβ, notable among them its spontaneous aggregation behavior, are extremely sensitive to the presence of trace amounts of fibrils, seeds, and nonsedimenting oligomers often present in commercial samples. The solution of Aβ, prepared as described in the Experimental Section, was free from seeds or other amyloidogenic material, as verified by its reproducible aggregation behavior and by the absence of bands other than that corresponding to the peptide when it was visualized by SDS-PAGE (Figure 1). In the obtained peptide solution, under nonstirring conditions, pH 7.4, and room temperature, no apparent aggregates were observed after periods of greater than 1 week.

Figure 2 shows the variation of surface pressure (surface tension of solvent minus the surface tension of any solution) for several peptide concentrations. The value was recorded 1500

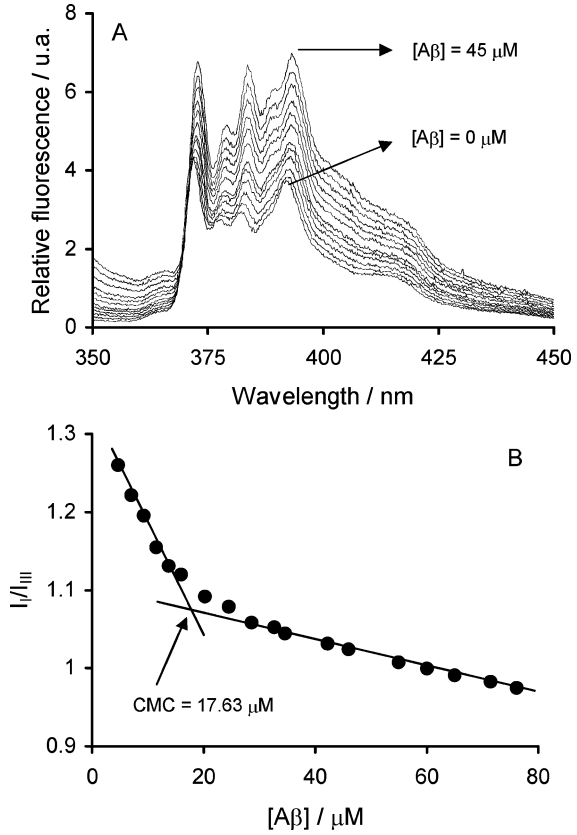

Figure 3. (a) Emission fluorescence spectra of a 10^{-7} M solution of pyrene at 25 °C at peptide concentrations ranging from 0 to 45 μM. Pyrene was excited at 334 nm, and the excitation and emission slits were 8 and 2 nm, respectively. (b) Ratio of vibronic band intensities I_I/I_{III} as a function of peptide concentration. Each point is the mean value of three measurements.

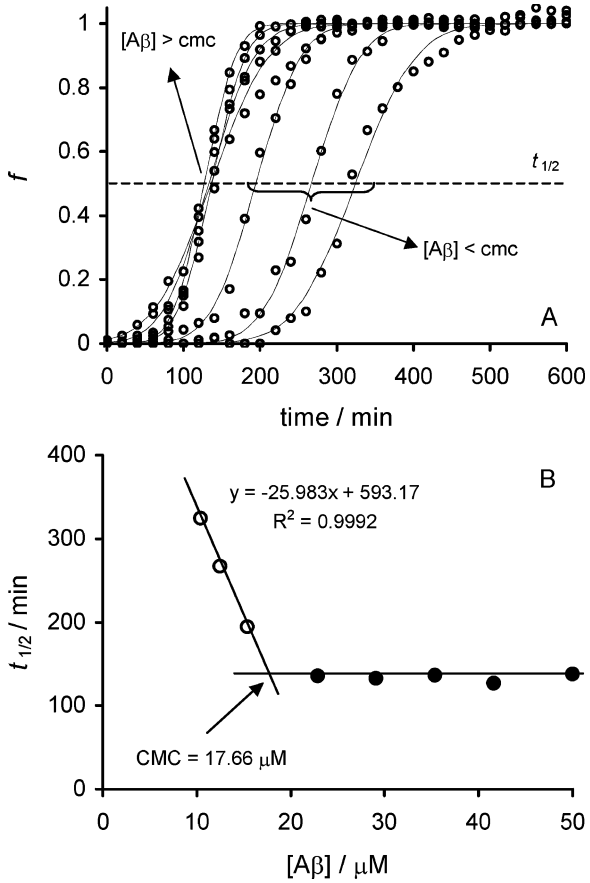

Figure 4. (a) Curves of aggregation of Aβ as a function of peptide concentration (from 10 to 50 μM). (b) Time of half-aggregation as a function of the above peptide concentrations.

s after addition of the peptide (time needed to reach equilibrium). We observed an ability of Aβ to lower the surface tension of water. Increasing concentrations of Aβ progressively lowered the surface tension (or in other words, increased the surface pressure). The CMC was determined from the peptide concentration at which the surface pressure became stable. We obtained a value of 17.5 μM. As indicated above, the CMC was also determined by fluorescence measurements. Figure 3a shows the emission fluorescence spectra for pyrene excited at 334 nm at peptide concentrations ranging from 0 to 45 μM in buffer peptide solutions. It is of paramount importance to keep the pyrene concentration low enough to prevent excimer formation. In the absence of micelles, pyrene senses the polar environment of water molecules, and the ratio of the fluorescence emission intensities corresponding to the first and third vibrational peaks (I_I/I_{III}) is high. Above the CMC and owing to the high hydrophobicity of pyrene molecules, these are solubilized in the micellar phase. As now the environment sensed by pyrene is less polar, the ratio I_I/I_{III} decreases. When the ratio between both these bands was recorded as a function of peptide concentration (Figure 3b), two slopes were obtained. The intercept of such slopes, at 17.6 μM, was assumed to be the value of the CMC.

To determine the aggregation number of the micelles, a 95 μM peptide concentration and seven quencher concentrations ranging from 0 to 20 μM were used. In absence of quencher, a fluorescence intensity (I_0) at 338 nm was obtained. When the quencher concentration was increased, lower values of fluorescence intensity (I_Q) were recorded. According to eqs 3 and 4, an aggregation number of 25 was obtained. As micelles of low aggregation number are more polydispersed than micelles of high aggregation number, the calculated value must be considered an average aggregation number. To obtain the associated error, we have determined the polydispersity index from eq 5. From this value (0.12), we obtained the standard deviation, and therefore, $N = 25 \pm 3$.

Determination of the fraction of fibrils formed as a function of peptide concentration (Figure 4a) allowed us to calculate the kinetic parameters of aggregation using eq 6. The obtained curves were sigmoidal in shape and rasemble those that are frequently reported for protein aggregation; at early times, there is a lag, followed by a phase of rapid increase of peptide in fibrils formed and then a plateau. In this way, using peptide concentrations ranging from 10 to 50 μM, we determined the times that define the kinetics (lag time, time of endpoint amplitude, and time of half-aggregation) for any concentration. We observe that at low concentrations an increase in the peptide concentration causes a reduction in the length of the lag phase. However, above a certain concentration, the curves are almost exactly overlapped. The independence of the aggregation behavior above a determined concentration is shown clearly in Figure 4b, which displays the variation in the time of half-aggregation as a function of peptide concentration. The representation is biphasic; at peptide concentrations below the CMC, the time of half-aggregation was dependent upon the initial amount of Aβ, whereas above this value the time of half-aggregation remained constant at 120 min. The peptide concentration above which the behavior changed was found by the intersection of the best straight lines through the two branches of the time−concentration curve, and this value was 17.7 μM, the same value as found above for the CMC.

Discussion

Elucidation of the kinetic pathway by which the monomer is converted to fibril has occupied the attention of several research groups. Besides the existence of monomers and fibrils, the published literature on amyloid fibril formation reports the existence of dimers, higher-order oligomers, and protofibrils.[25] Concerning Aβ fibrillogenesis, the nucleation−elongation model represents the school of thought more generally accepted. In this model, initial self-assembly is slow and unfavorable until a critical size is reached. Once the nucleus is formed, further elongation by the addition of monomers is rapid. Hence, nucleation is rate-limiting for amyloidogenesis. The rate of aggregation is expected to have a high-order dependence (where the order is related to the number of monomers that contain a nucleus) on the concentration of peptide. Lomakin et al.[7] proposed a detailed mathematical model for the fibrillogenesis of Aβ, including the presence of micelles. These are in rapid equilibrium with monomers, and from micelles the nuclei are spontaneously and irreversibly generated. Soreghan et al. suggested for the first time that Aβ peptides organized within the amyloid fibril in the same fashion as surfactant molecules organized in micelles.[10]

Using some of the most appropriate physicochemical techniques employed to characterize micelles, namely, surface pressure and fluorescence measurements, we have measured a CMC of 17.6 ± 0.1 μM for Aβ (1−40) in 10 mM Tris, pH 7.4, and 5% (v/v) DMSO. It is remarkable that we have obtained the same CMC value within the experimental error of the measurements by means of two independent techniques. Although Soreghan et al.[10] had already indicated a CMC of 25 μM for several Aβ analogues (this group used a wider concentration range than us, which explains the difference between their value and ours), a CMC ranging from 10 to 40 μM has been generally accepted.[26] To provide insight into the characteristics of such micelles, the aggregation number has been determined. We have obtained a value of 25 ± 3, which is consistent with the value reported by Yong et al.,[13] who by means of SANS experiments confirmed that upon dissolution, under acidic conditions, and at a concentration above 0.15 mg mL^{-1} Aβ monomers form micellelike aggregates consisting of about 30 monomers.

The existence of micelles implies that the nucleation−polymerization mechanism[5] as a model for explaining the Aβ fibrillogenesis must be revised. It can no longer be applied, at least at supramicellar peptide concentrations, since the most outstanding feature of this model is the strong concentration dependence of the nucleation rate, r_n, given through $r_n \approx C_P^n \approx 1/t_{lag}$ (lag time). The exponent n denotes the number of monomers building up the nucleus. Hence, the lag time should decrease exponentially with increasing soluble protein concentration, even for nuclei consisting of only a few monomers, which is not the case, as we have observed experimentally (Figure 4). We found that for a peptide concentration above 17.7 μM the lag time (or the time of semiaggregation) was independent of the total concentration of the peptide, directly contradicting the predictions of the model described. That is, the aggregation of Aβ does not show a high-order dependence on the concentration of monomeric peptide. However, the concentration at which the aggregation time of Aβ becomes concentration-independent coincides with the CMC values obtained by surface pressure or fluorescence measurements, further supporting the role of micelles in fibrillogenesis. Once the existence of micelles has been clearly demonstrated, an important factor affecting micelles in fibrillogenesis is whether they are on- or off-pathway. Lomakin et al.[7] differentiate two mechanisms of fibrillogenesis depending upon whether the total protein concentration is above or below a certain critical level. They affirm that when the concentration is above this critical concentration (which must correspond with the CMC) the initial rate of elongation is independent of the concentration. This would mean that the kinetics of the process could be assumed to be a zero-order reaction, and if the rate of elongation was independent of concentration, then the time needed to convert a predetermined amount of the material into fibrillar form would be proportional to concentration and not independent of concentration as we have observed experimentally. We think that these authors would want to say exactly quite the reverse, because their model, developed in that and in other papers, is quantitatively excellent.[6,7,13]

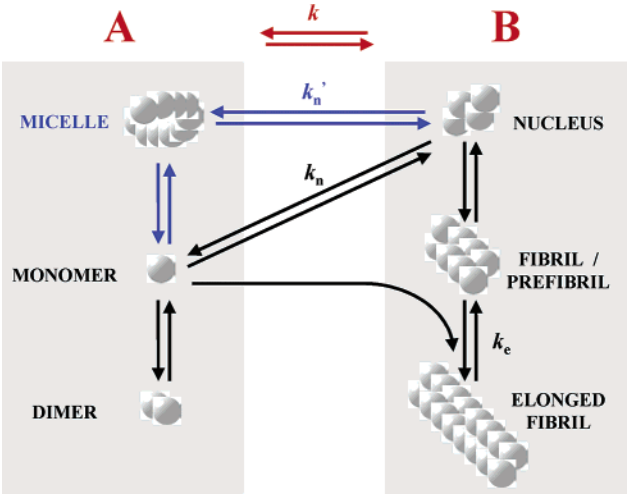

Figure 5. Schematic representation of the location and function of micelles in the model of fibrillogenesis of amyloid β peptide. The overall reaction can be thought of as the conversion of peptide monomer into fibrils by means of a reaction of an apparent first-order. The number of individual steps in the nucleation and growth phases is not specified in this model. When the concentration exceeds the CMC, the nuclei can originate from the micelles, and this pathway predominates over the nucleation from monomers, which is the rate-limiting step at submicellar peptide concentrations. In this model, micelles are directly related to nuclei (and, in consequence, with fibrils). At supramicellar concentrations, an increase in peptide concentration implies an increase in micelle concentration and, therefore, an increase in the amount of nuclei and then in short fibrils (or prefibrils) and fibrils. Under these conditions, all of the steps along the pathway are energetically favorable.

The fact that above the CMC the kinetic curves are universal, independent of the total peptide concentration, allows us to confirm the location of the micelles in the fibrillogenesis. We can state that there are basically two entities: (A) monomers, dimers, and micelles all in fast equilibrium and (B) fibrils, including the shortest of them, nuclei. A is slowly converted to B. (Figure 5). The peptide concentration and the concentration of the micelles are related according to the principles of thermodynamic equilibrium between monomers and micelles. Above the CMC, the concentration of monomers and small oligomers is essentially constant, and as the total concentration of the peptide changes, only the concentration of the micelles changes, since whenever the total peptide concentration exceeds the CMC all excess peptide is incorporated into micelles, which act as a monomer reservoir. Hence, above the CMC, the concentration of micelles is proportional to the total peptide concentration, and the formation of monomers from micelles can be considered as a zero-order reaction. The conversion of A to B involves two processes, creation of new fibrils

(nucleation) and elongation of existing fibrils (elongation). The process of elongation is produced by the attachment of monomers and/or oligomers to existing fibrils. In this way, the total rate of conversion is k_e[F][M], where [F] is the concentration of fibrils and [M] is the concentration of monomers and/or oligomers, which is constant above the CMC. Thus, the total conversion rate, r, will depend only on the concentration of the fibrils

$$r = k[\mathrm{F}] \tag{7}$$

where k is the product of the elongation constant, k_e, with the monomer concentration, [M], which is the CMC.

Hence, as the conversion of A into fibrils is concerned, we can think of a simple model consisting of a reactant A (formed by monomers, dimers, or other oligomers, and micelles) and of a product B (nuclei and fibrils). The conversion of A into B follows the kinetics of an apparent first-order reaction, and this explains why the time of the half-aggregation does not exhibit any kind of dependence upon the total protein concentration. At micellar concentrations, the rate-limiting step seems to be bypassed.

In order for the kinetic curves to be universal, when the rate of elongation is constant, [F] must scale as peptide concentration, as micelles do. In consequence, [F] must to depend on the micelle concentration Thus, the conversion rate must be variable and depend on the concentration. In other words, micelles can serve as the nucleation centers. In this situation, the number of fibrils formed will be proportional to the peptide concentration, and since all fibrils grow with the same elongation rate, the overall conversion rate will be proportional to the peptide concentration. Thus, the role of the micelles in the fibrillogenesis only can be explained if the micelles are located on-pathway.

Thus, the model based in a classical nucleation-dependent polymerization must be revised. It is possible that nuclei and intermediates or oligomers are closely related and that the rate-limiting step is actually a conformational conversion. Recently, Kelly's group[27] have shown that the fibrillogenesis of a monomeric variant of transthyretin is incompatible with the expectations for a nucleation-dependent polymerization, since they have found that the dependence of the reaction time course is first-order on the transthyretin concentration. While the existence and/or the location of micelles in the fibrillogenesis may not be important in screening for compounds that inhibit fibril assembly, it is nevertheless important to understand the mechanism of amyloid assembly.

Conclusions

The existence of micelles in the fibrillogenesis of Aβ has been shown, since the physicochemical behavior of this peptide changes above a determined peptide concentration. By accurate experimental determinations, we have obtained a CMC of 17.5 μM (surface tension equilibrium) and of 17.6 μM (changes in the fluorescence of pyrene). Using a classical fluorescence technique, we have obtained an aggregation number $N = 25 \pm 3$.

The time of half-aggregation was independent of concentration above 17.7 μM, a fact that confirms, again, that above 17.6 $\pm$ 0.1 μM Aβ clusters in a micellar form. Above this concentration, the kinetic conversion of peptide monomers into fibrils can be considered an apparent first-order reaction. To maintain the universality of the kinetic curves above the CMC, a direct connection between micelles and nuclei must exist, and consequently, micelles must be on-pathway of the fibrillogenesis.

Acknowledgment. This research was supported in part by the Spanish Ministerio de Sanidad y Consumo (FIS 00/1121). R.S. received a grant (00337 APSQV) from CIRIT (Generalitat de Catalunya). The authors thank Sandra Merino for her experimental skill in SDS-PAGE.

References and Notes

(1) Iqbal, K. Prevalence and neurobiology of Alzheimer's disease. In *Alzheimer's Disease: Basic Mechanism, Diagnosis and Therapeutic Strategies*; Iqbal, K., McLachlan, D. R. C., Winblad, B., Winsniewski, H. M., Eds.; John Wiley and Sons: New York, 1991; pp 1−5.
(2) Hardy, J. *Trends Neurosci.* **1997**, *20*, 154.
(3) Koo, E. H.; Lansbury, P. T., Jr. *Proc. Natl. Acad. Sci. U.S.A.* **1999**, *96*, 9989.
(4) Soto, C. *FEBS Lett.* **2001**, *498*, 204.
(5) Jarrett, J. T.; Lansbury, P. T., Jr. *Cell* **1993**, *73*, 1055.
(6) Lomakin, A.; Chung, D. S.; Benedek, G. B.; Kirschner, D. A.; Teplow, D. B. *Proc. Natl. Acad. Sci. U.S.A.* **1996**, *93*, 1125.
(7) Lomakin, A.; Teplow, D. B.; Kirschner, D. A.; Benedek, G. B. *Proc. Natl. Acad. Sci. U.S.A.* **1997**, *94*, 7942.
(8) Teplow, D. B. *Amyloid* **1998**, *5*, 121.
(9) Gazit, E. *Angew. Chem., Int. Ed.* **2002**, *41*, 257.
(10) Soreghan, B.; Kosmoski, J.; Galbe, C. *J. Biol. Chem.* **1994**, *269*, 28551.
(11) Walsh, D. M.; Lomakin, A.; Benedek, G. B.; Condron, M. M.; Teplow, B. *J. Biol. Chem.* **1997**, *272*, 22364.
(12) Naiki, H.; Nakakuki, K. *Lab. Invest.* **1996**, *74*, 374.
(13) Yong, W.; Lomakin, A.; Kirkitadze, M. D.; Teplow, D. B.; Chen, S.-H.; Benedek, G. B. *Proc. Natl. Acad. Sci. U.S.A.* **2002**, *90*, 150.
(14) Kayed, R.; Head, E.; Thompson, J. L.; McIntire, T. M.; Milton, S. C.; Cotman, C. W.; Glabe, C. G. *Science* **2003**, *300*, 486.
(15) Phillips, J. N. *Trans. Faraday Soc.* **1955**, *51*, 561.
(16) Maget-Dana, R. *Biochim. Biophys. Acta* **1999**, *1462*, 109.
(17) Aguiar, J.; Carpena, P.; Molina-Bolívar, J. A.; Carnero Ruiz, C. *J. Colloid Interface Sci.* **2003**, *258*, 116.
(18) Infelta, P. P.; Grätzel, M.; Thomas, J. K. *J. Phys. Chem.* **1974**, *78*, 190.
(19) Tachiya, M. *Chem. Phys. Lett.* **1975**, *33*, 289.
(20) Turro, N. J.; Yekta, A. *J. Am. Chem. Soc.* **1978**, *100*, 5951.
(21) Stam, J.; Depaemelaere, S.; De Schryver, F. C *J. Chem. Educ.* **1998**, *75*, 93.
(22) Warren, G. G.; Grieser, J. *Chem. Soc., Faraday Trans. 1* **1986**, *82*, 1813.
(23) Kahimira, M.; Naito, A.; Tuzi, S.; Nosaka, A. Y.; Saito, H. *Protein Sci.* **2000**, *9*, 867.
(24) Sabaté, R.; Gallardo, M.; Estelrich, J. *Biopolymers* **2003**, *71*, 190.
(25) Roher, A. E.; Baudry, J.; Chaney, M. O.; Kuo, Y. M.; Stine, W. B.; Emmerling, M. R. *Biochim. Biophys. Acta* **2000**, *502*, 31.
(26) Harper, J. D.; Lansbury, P. T., Jr. *Annu. Rev. Biochem.* **1997**, *66*, 385.
(27) Hurshman, A. R.; White, J. T.; Powers, E. T.; Kelly, J. W. *Biochemistry* **2004**, *43*, 7365.